Supporting Information

Enhanced Polymer Crystallinity in Mixed Matrix Membranes Induced by Metal–Organic Framework Nanosheets for Efficient CO_2 Capture

Youdong Cheng,[†] Sérgio R. Tavares,[‡] Cara M. Doherty,[§] Yunpan Ying,[†] Erik Sarnello,[∥] Guillaume Maurin,[‡] Matthew R. Hill,[§,⊥] Tao Li,[∥,#] and Dan Zhao[,†]*

[†] Department of Chemical and Biomolecular Engineering, National University of Singapore, 4 Engineering Drive 4, Singapore 117585

[‡] Institut Charles Gerhardt Montpellier, Université de Montpellier, Place E. Bataillon, Montpellier Cedex 05, 34095, France

[§] CSIRO Manufacturing, Private Bag 10, Clayton South, Victoria 3169, Australia

[∥] Department of Chemistry and Biochemistry, Northern Illinois University, DeKalb, IL 60115, USA

[⊥] Department of Chemical Engineering, Monash University, Clayton, Victoria 3800, Australia

[#] X-Ray Science Division, Advanced Photon Source, Argonne National Laboratory, Argonne, IL 60439, USA

*E-mail: chezhao@nus.edu.sg (D.Z.)

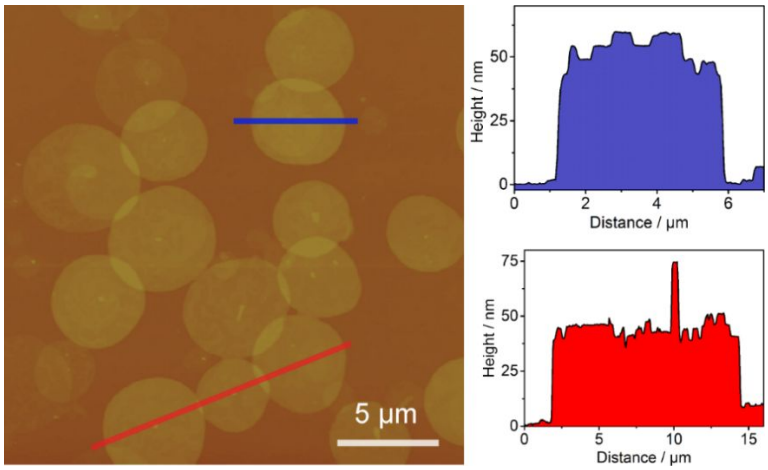

Figure S1. Additional AFM image of NUS-8 nanosheets.

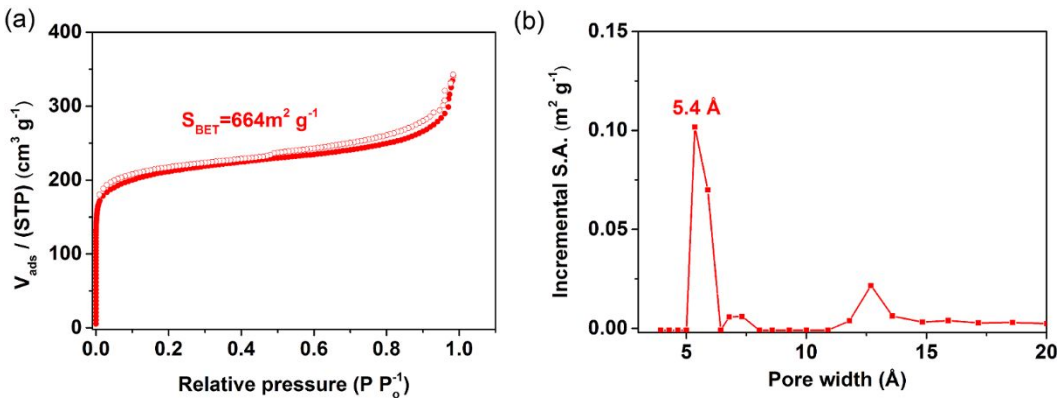

Figure S2. (a) Nitrogen sorption isotherms at 77 K of NUS-8 nanosheets. (b) Pore size distribution of NUS-8 nanosheets calculated by nonlocal density functional theory based on slit pore model.

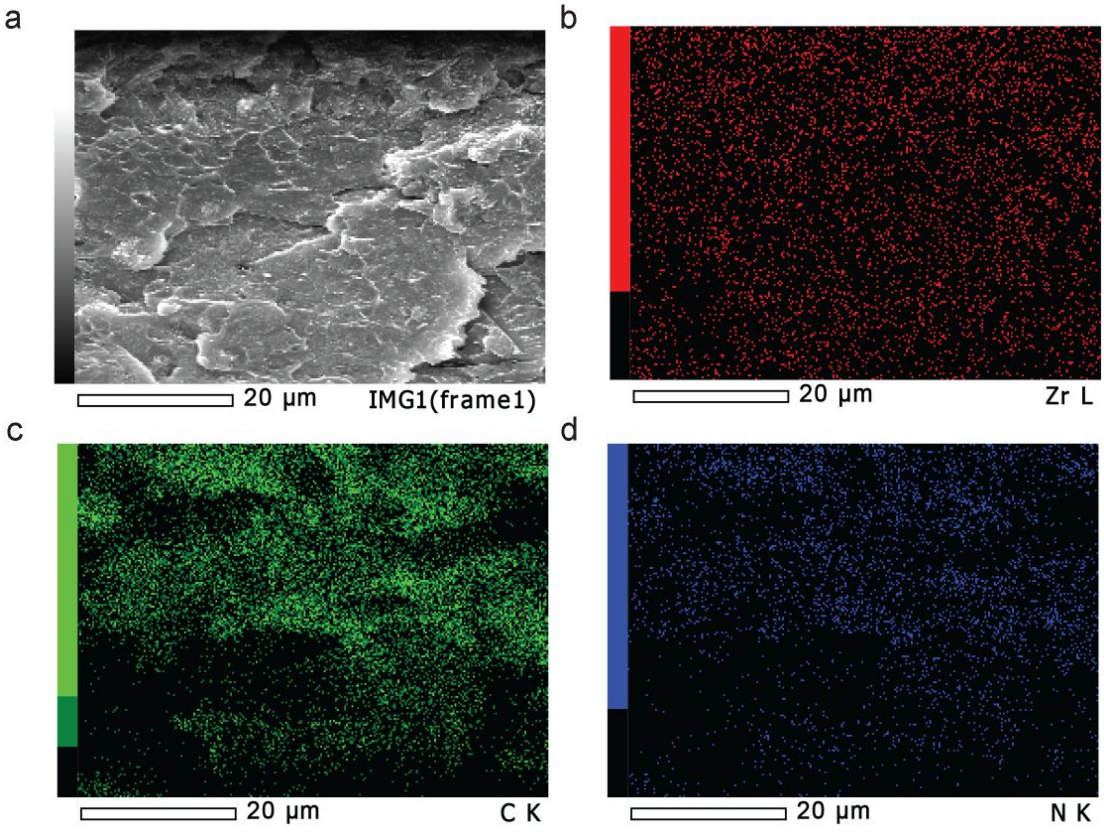

Figure S3. (a) FESEM image of MMMs with 2 wt% of NUS-8. EDX element mapping of zirconium (b), carbon (c) and nitrogen (d) in the FESEM image. Zirconium only exists in NUS-8 and its homogeneous distribution in the EDX mapping shows the good dispersion of NUS-8 inside the PIM-1 matrix.

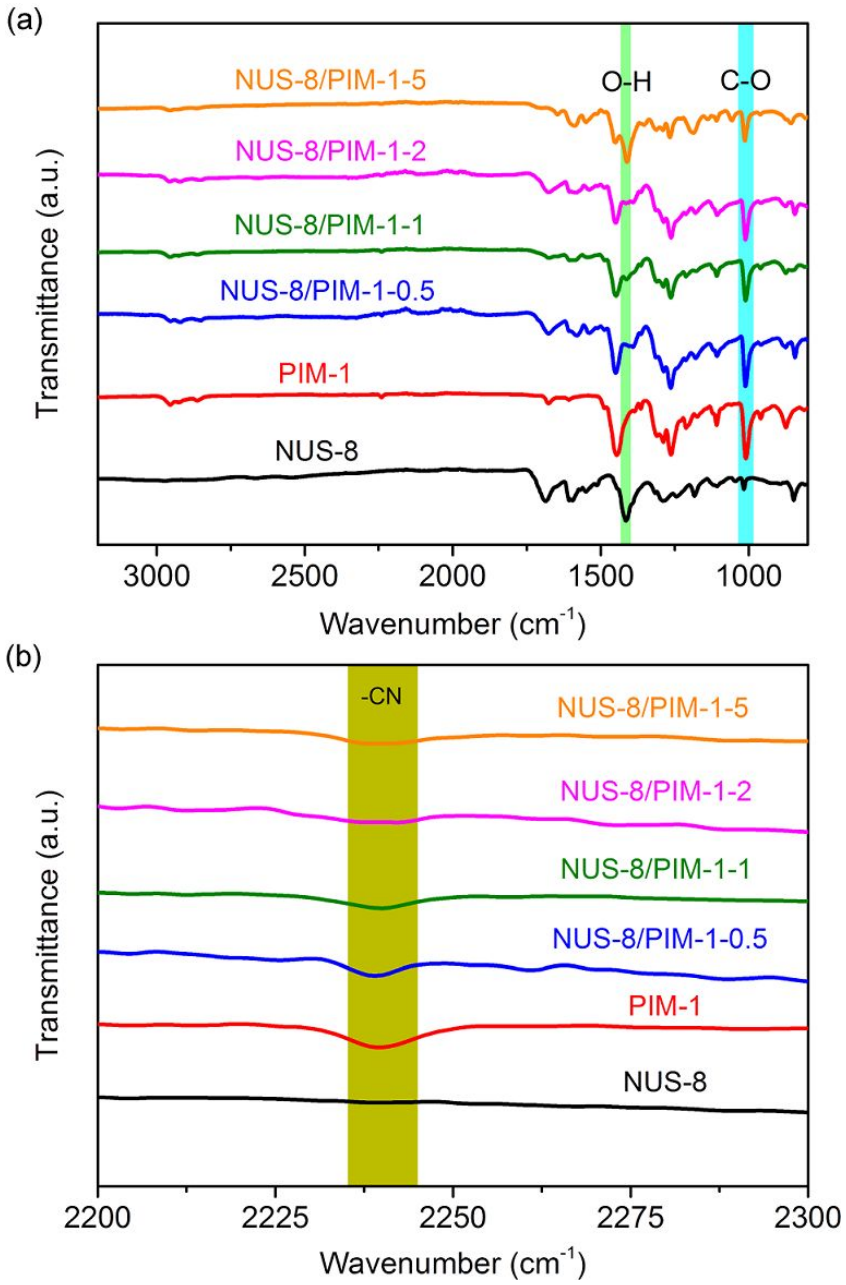

Figure S4. (a) FTIR spectra of pure NUS-8, pure PIM-1 membrane and NUS-8/PIM-1 MMMs. (b) Enlarged FTIR spectra for all samples, showing that nitrile groups (-CN) exhibit a decreased adsorption intensity after the incorporation of NUS-8.

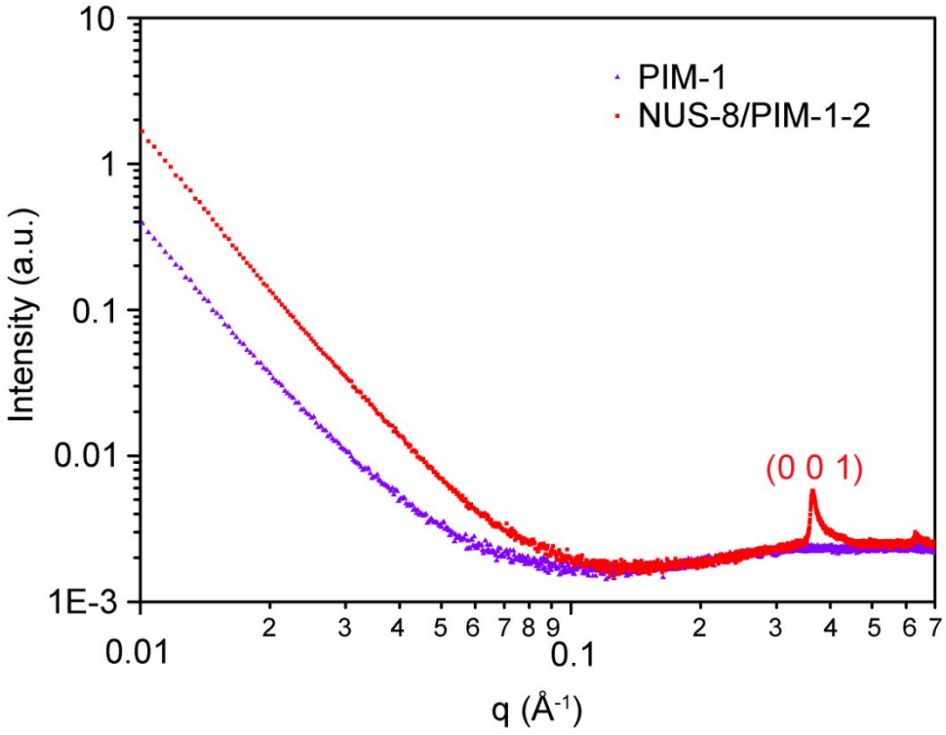

Figure S5. SAXS patterns of pure PIM-1 membrane and NUS-8/PIM-1-2 MMM, showing the preservation of MOF crystallinity during the membrane fabrication.

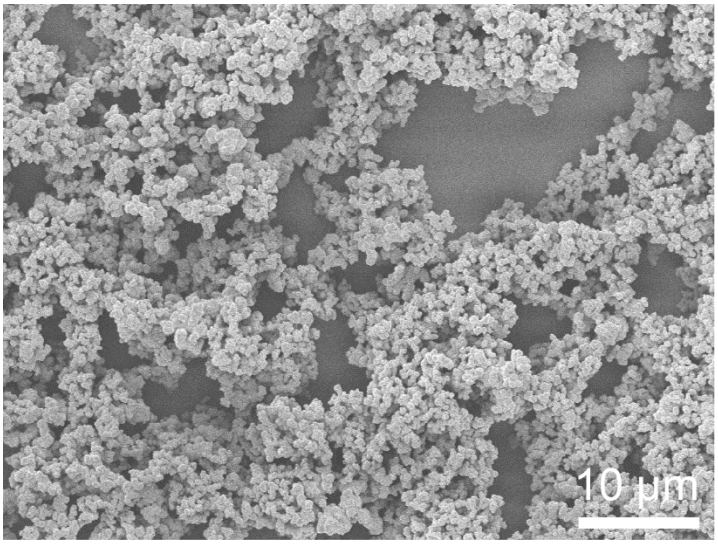

Figure S6. FESEM image of UiO-66-NH_2 nanoparticles.

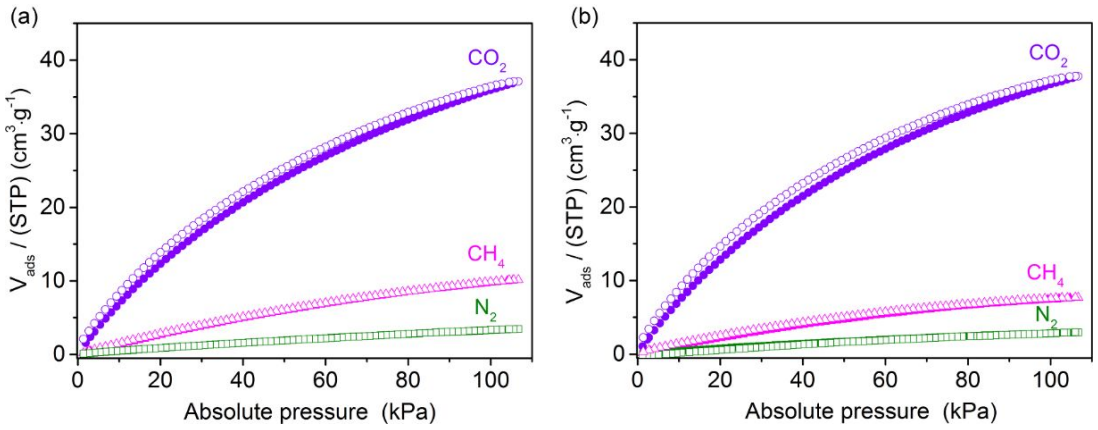

Figure S7. CO_2, CH_4 and N_2 uptakes of (**a**) pure PIM-1 membrane and (**b**) NUS-8/PIM-1-2 MMM at 25 °C.

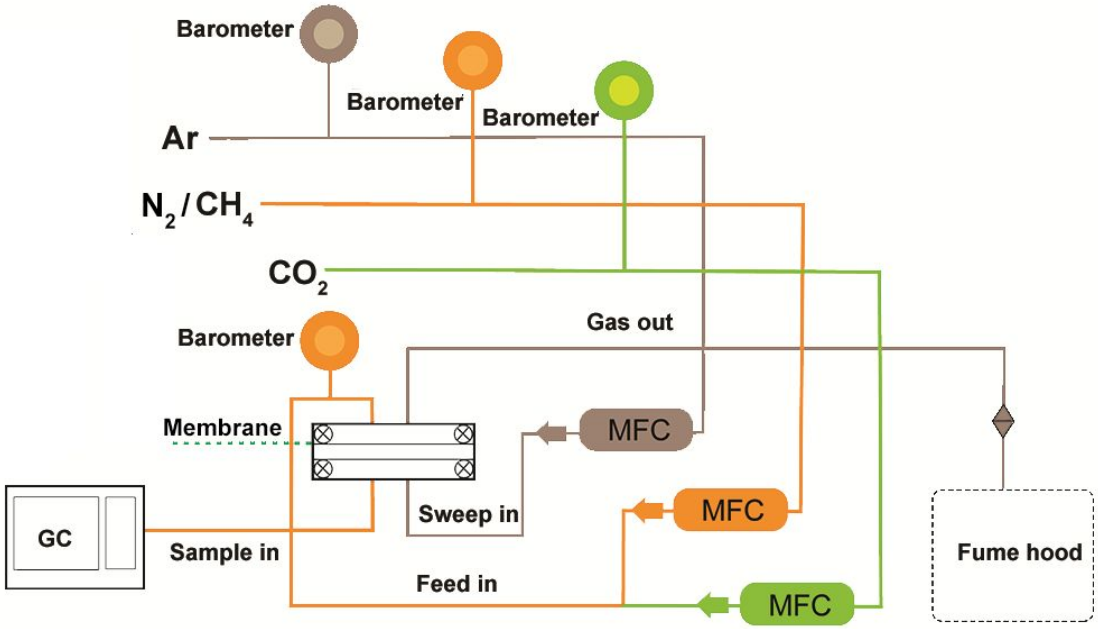

Figure S8. The scheme of the homo-made membrane testing set up used in this study.

Table S1. PALS parameters measured for pure PIM-1 membrane and NUS-8/PIM-1-2 MMM.

Membrane type	τ_3 (ns)	I_3 (%)	τ_4 (ns)	I_4 (%)	R_3 (Å)	R_4 (Å)
Pure PIM-1	1.730±0.121	5.3±0.2	5.281±0.154	15.8±0.4	0.518±0.025	0.975±0.014
NUS-8/PIM-1-2	1.564±0.101	5.6±0.1	4.959±0.031	15.1±0.3	0.483±0.023	0.945±0.003

Table S2. Gas separation performance of pure PIM-1 membrane and NUS-8/PIM-1 MMM measured at 298 K with a transmembrane pressure of 1 bar.

Membrane type	Membrane thickness (μm)	CO_2/CH_4			CO_2/N_2		
		CO_2 permeability (Barrer)	CH_4 permeability (Barrer)	CO_2/CH_4 selectivity	CO_2 permeability (Barrer)	N_2 permeability (Barrer)	CO_2/N_2 selectivity
Pure PIM-1	58±7	4020±38	288±3.6	13.9±0.25	3895±61	231±6.7	15.6±0.25
NUS-8/PIM-1-0.5	63±12	4855±176	274±13	17.8±0.50	4958±125	282±8	16.6±0.45
NUS-8/PIM-1-1	71±6	5202±43	211±11	24.6±0.95	5145±128	226±4.4	22.6±1.01
NUS-8/PIM-1-2	66±12	6462±89	217±8.4	30.1±0.46	6725±210	252±19.6	26.8±1.7
NUS-8/PIM-1-5	75±7	8670±86	463±4.6	18.7±0.7	8288±104	389±8	21.3±0.4

Table S3. Overview of commercially available polymeric membranes and representative PIM-1 based membranes for CO_2/CH_4 separation.

Membrane type	Separation performance		Operation conditions			Reference
	CO_2 permeability (Barrer)	CO_2/CH_4 selectivity	Temperature (°C)	Pressure (bar)	Feed gas type	
Cellulose acetate	6.0	29	35	0.27	Pure	1
Polycarbonate	8.8	23.6	25	3.6	Pure	2
Matrimid®	9.6	34.5	35	1	Pure	3
Polysulfone	5.4	31.1	35	1.75	Mixed	4
Polyphenyleneoxide	58.0	14.3	35	10	Pure	5
TOX-PIM-1	1100	69	22	4	Pure	6
UV-PIM-1	1364	31	22	4	Pure	7
ZIF-8/PIM-1	19350	7.5	22	1	Pure	8
CC3/PIM-1	18090	14	25	1	Pure	9
Silicate 1/PIM-1	2530	13	25	1	Pure	10
NUS-8/PIM-1	6462	30.1	25	1	Mixed	This work

Table S4. Overview of commercially available polymeric membranes and representative PIM-1 based membranes for CO_2/N_2 separation.

Membrane type	Separation performance		Operation conditions			Reference
	CO_2 permeability (Barrer)	CO_2/N_2 selectivity	Temperature (°C)	Pressure (bar)	Feed gas type	
Cellulose acetate	6.0	25.8	35	27	Pure	11
Polydimethylsiloxane	2317	10.8	28	\	Pure	12
Matrimid®	8.2	28.5	25	1.4	Pure	13
Polysulfone	4.46	24.8	35	4	Pure	14
TOX-PIM-1	1100	37	22	4	Pure	6
UV-PIM-1	1364	32.4	22	4	Pure	7
SNW-1/PIM-1	5236	18.9	30	2	Mixed	15
UiO-66-NH_2/PIM-1	2005	22	25	4	Pure	16
HCP/PIM-1	10040	17.1	25	2	Pure	17
NUS-8/PIM-1	6725	26.8	25	1	Mixed	This work

Table S5. Comparisons of membrane performance change in MMMs containing different porous fillers.

Polymer	Filler	Filler loading (%)	Filler pore size (Å)	Performance change (%)		Reference
				P_{CO_2}	$S_{(CO_2/gas)}$	
PIM-1	ZIF-67	20	~3.4	+18	+30[a]	18
6FDA-based PI	ZIF-8@PD	30	3.4	+270	-43[a]	19
6FDA-DAM	ZMOF	20	4.5	+55	+35[a]	20
6FDA-DAM	Y-fum-fcu-MOF	30	~4.7	+42	+20[a]	21
PSF	SNW-1	12	5	+148	+89[a]	22
PIM-1	CuBDC	4	5.4	-26	+29[a]	23
PEO	UiO-66-MA	2	~6	+293	-6[b]	24
PIM-1	UiO-66-NH_2	10	~6	+95	-6[a]	16
6FDA−DAM	MOP-15	1.6	6	+40	+12[b]	25
Pebax®	ZIF-300	30	7.9	+65	+58[b]	26
Matrimid®	MIL-53-NH_2	25	~8	+87	+19[a]	27
Ultem	NUS-2	10	8	+93	+61[a]	28
PEI	C-MOF-5	25	8.7	+221	+25[a]	29
6FDA-DAM	ZIF-94	40	9.1	+148	-9[b]	30
Matrimid®	ACOF-1	16	9.4	+125	+6[a]	31
PIM-1	MOF-74	20	11	+223	+53[b]	32
PBI-BuI	TpPa-1	40	18	+117	-19[a]	33
Pebax®	MCM-41	20	27	+53	~0[a]	34
PIM-1	NUS-8	2	6	+73	+117[a]	This work
PIM-1	NUS-8	2	6	+61	+72[b]	This work

Gas separation data were obtained for a. CO_2/CH_4 separation; b. CO_2/N_2 separation.

Supplementary Note 1: Modelling of the NUS-8/PIM-1 interface.

The NUS-8 structure was first geometry-optimized at the Density Functional Theory level using the Quantum ESPRESSO package,[35] which implements DFT with periodic boundary conditions and plane wave functions as basis sets. These calculations were performed with the generalized gradient approximation (GGA/PBE)[36] while the ion cores were described by Vanderbilt pseudopotentials[37] and the Kohn-Sham one electron states were expanded in a plane wave basis until the kinetic cutoff energy was equal to 40 Ry (400 Ry for the density). The relative ion positions were relaxed until all the force components were lower than 0.001 Ry $Bohr^{-1}$. As a further step, a supercell made of (2 × 2 × 1) unit cell, containing 2016 atoms was considered to further accommodate the dimension of PIM-1. Each atom of NUS-8 was considered as a single charged Lennard-Jones (LJ) site with LJ potential parameters taken from UFF and DREIDING for the inorganic and organic nodes respectively while the charges were calculated using a ESP scheme applied to the cluster cut from the periodic structure.[38,39] The atomistic model of PIM-1 was built following the previously reported strategy based on the use of the codes Lammps and Polymatic.[40-42] PIM-1 was modelled by an united atom model where its flexibility was treated by the consideration of intra-molecular terms including harmonic bonding and bending contributions, while cosine-based functions were used to model the torsion modes. The corresponding parameters were taken from the GAFF force field.[43] In the case of the non-bonded contributions, 12-6 LJ and Coulomb potentials were used, with LJ parameters extracted from TraPPE force field and ESP charges obtained from

DFT calculations.[44] The table S6 summarizes the charges extracted for NUS-8, with the labels of the atoms reported in Figure S9. The complete list of LJ parameters and atomic partial charges of the PIM-1 model is provided in our previous study.[45]

Table S6. ESP Charges for the NUS-8 model.

Atom Label	Charge
Zr	+2.303
O1	-0.713
O2	-1.126
O3	-1.201
O4	-0.965
H1	+0.159
H3	+0.534
H4	+0.459
C1	+0.936
C2	+0.001
C3	-0.182

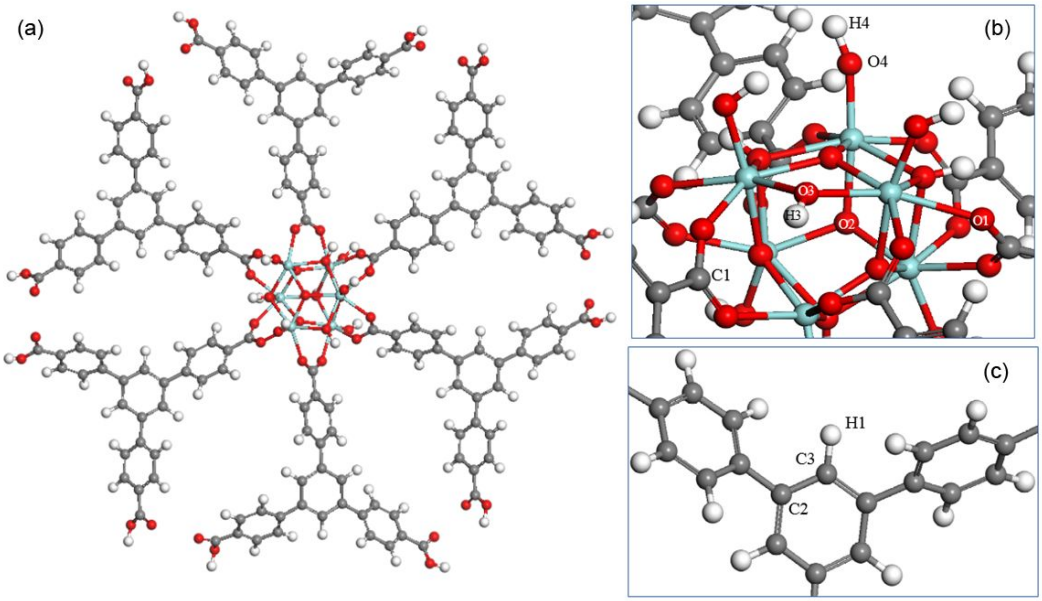

Figure S9. (a) Adopted cluster model for the computation of the ESP charges. Overview of the inorganic node (b) and the organic linker (**c**) with their respective atom labels. Color code: Zr (light blue), O (red), C (gray) and H (white).

The interface was finally modelled by means of a methodology previously developed by some of us.[40] The MOF and polymer components were first equilibrated and then the simulation boxes were brought together resulting in a final box with 40.6 × 67.27 × 160 $Å^3$ size: taken from our previous study.[45] This composite system was equilibrated by seven cycles of molecular dynamics (MD) simulations, each of them consisting of two simulations in the NVT ensemble and one in the NP_nT ensemble, where P_n corresponds to the pressure component in the z direction, the direction normal to the interface. The first and second simulations of each cycle were performed at 600 K and 300 K, respectively. The pressure was increased until 50 kbar and then gradually decreased to 1 bar. After this equilibration step, data were

collected from four statistically independent simulations, each one lasting 10 ns, with a time step of 1 fs. The Berendsen thermostat and barostat were used with relaxation times of 0.1 and 0.5 ps, respectively.[46] The interface generation and the production stage were performed using a modified version of DLPOLY classic.[47] The MOF/Polymer interactions were treated using the sum of a LJ potential term and a coulombic contribution. The crossed LJ interactions were computed by the Lorentz-Berthelot mixing rules.[48] A cutoff was set to 15 Å to calculate the van der Waals interactions while the coulombic interactions were computed using the Ewald summation method.[48]

Supplementary Note 2: Positron annihilation lifetime spectroscopy tests.

Positron annihilation lifetime spectroscopy (PALS) was used to determine the average size of the free volume elements in pure PIM-1 and 2 wt% MMM. The membranes were cut to 1 cm^2 and stacked into 3 mm bundles. The positron source ($^{22}NaCl$ sealed in Mylar envelope) was placed in the middle of the membrane bundle and the lifetimes were collected for 24 hours under vacuum (10^{-6} torr) using two EG&G Ortec Spectrometers with a resolution function of 260 ps. A minimum of five spectra with 4.5×10^6 integrated counts was collected and analyzed using LT-v9 software.[49] The spectra were fitted to 4 lifetime components and a source correction (1.486 ns and 3.6%). The first component, due to p-Ps annihilation, was fixed to 0.125 ns and the second component ~0.4 ns was attributed to free annihilation. The third and fourth component were attributed to o-Ps annihilation and their lifetimes were used to calculate the average pore sizes for the bimodal distribution using the Tao-Eldrup

equation.[50,51] The pore size distribution representation was performed using PAScual software.[52]

References

(1) Scholes, C. A.; Stevens, G. W.; Kentish, S. E. Membrane Gas Separation Applications in Natural Gas Processing. *Fuel* **2012**, *96*, 15–28.

(2) Şen, D.; Kalıpçılar, H.; Yilmaz, L. Development of Polycarbonate Based Zeolite 4A Filled Mixed Matrix Gas Separation Membranes. *J. Membr. Sci.* **2007**, *303*, 194–203.

(3) Bachman, J. E.; Long, J. R. Plasticization-Resistant Ni_2(dobdc)/Polyimide Composite Membranes for the Removal of CO_2 from Natural Gas. *Energy Environ. Sci.* **2016**, *9*, 2031–2036.

(4) Seoane, B.; Sebastian, V.; Tellez, C.; Coronas, J. Crystallization in THF: the possibility of one-pot synthesis of mixed matrix membranes containing MOF MIL-68(Al). *CrystEngComm* **2013**, *15*, 9483–9490.

(5) Rowlett, J. R.; Liu, Q.; Zhang, W.; Moon, J. D.; Dose, M. E.; Riffle, J. S.; Freeman, B. D.; McGrath, J. E. Gas Transport Properties and Characterization of UV Crosslinked Poly(Phenylene Oxide-co-Arylene Ether Ketone) Copolymers. *J. Mater. Chem. A* **2016**, *4*, 16047–16056.

(6) Song, Q.; Cao, S.; Pritchard, R. H.; Ghalei, B.; Al-Muhtaseb, S. A.; Terentjev, E. M.; Cheetham, A. K.; Sivaniah, E. Controlled Thermal Oxidative Crosslinking of Polymers of Intrinsic Microporosity towards Tunable Molecular Sieve Membranes. *Nat. Commun.* **2014**, *5*, 4813.

(7) Song, Q.; Cao, S.; Zavala-Rivera, P.; Ping Lu, L.; Li, W.; Ji, Y.; Al-Muhtaseb, S. A.; Cheetham, A. K.; Sivaniah, E. Photo-Oxidative Enhancement of Polymeric Molecular Sieve Membranes. *Nat. Commun.* **2013**, *4*, 1918.

(8) Bushell, A. F.; Attfield, M. P.; Mason, C. R.; Budd, P. M.; Yampolskii, Y.; Starannikova, L.; Rebrov, A.; Bazzarelli, F.; Bernardo, P.; Carolus Jansen, J.; Lanč, M.; Friess, K.; Shantarovich, V.; Gustov, V.; Isaeva, V. Gas Permeation Parameters of Mixed Matrix Membranes Based on the Polymer of Intrinsic Microporosity PIM-1 and the Zeolitic Imidazolate Framework ZIF-8. *J. Membr. Sci.* **2013**,

427, 48–62.

(9) Bushell, A. F.; Budd, P. M.; Attfield, M. P.; Jones, J. T. A.; Hasell, T.; Cooper, A. I.; Bernardo, P.; Bazzarelli, F.; Clarizia, G.; Jansen, J. C. Nanoporous Organic Polymer/Cage Composite Membranes. *Angew. Chem. Int. Ed.* **2013**, *52*, 1253–1256.

(10) Mason, C. R.; Buonomenna, M. G.; Golemme, G.; Budd, P. M.; Galiano, F.; Figoli, A.; Friess, K.; Hynek, V. New Organophilic Mixed Matrix Membranes Derived from a Polymer of Intrinsic Microporosity and Silicalite-1. *Polymer* **2013**, *54*, 2222–2230.

(11) Li, J.; Wang, S.; Nagai, K.; Nakagawa, T.; Mau, A. W. H. Effect of Polyethyleneglycol (PEG) on Gas Permeabilities and Permselectivities in its Cellulose Acetate (CA) Blend Membranes. *J. Membr. Sci.* **1998**, *138*, 143-152.

(12) Tantekin-Ersolmaz, Ş. B.; Atalay-Oral, Ç.; Tatlıer, M.; Erdem-Şenatalar, A.; Schoeman, B.; Sterte, J. Effect of Zeolite Particle Size on the Performance of Polymer-Zeolite Mixed Matrix Membranes. *J. Membr. Sci.* **2000**, *175*, 285–288.

(13) Venna, S. R.; Lartey, M.; Li, T.; Spore, A.; Kumar, S.; Nulwala, H. B.; Luebke, D. R.; Rosi, N. L.; Albenze, E. Fabrication of MMMs with Improved Gas Separation Properties Using Externally-Functionalized MOF Particles. *J. Mater. Chem. A* **2015**, *3*, 5014–5022.

(14) Kim, S.; Marand, E.; Ida, J.; Guliants, V. V. Polysulfone and Mesoporous Molecular Sieve MCM-48 Mixed Matrix Membranes for Gas Separation. *Chem. Mater.* **2006**, *18*, 1149–1155.

(15) Wu, X.; Tian, Z.; Wang, S.; Peng, D.; Yang, L.; Wu, Y.; Xin, Q.; Wu, H.; Jiang, Z. Mixed Matrix Membranes Comprising Polymers of Intrinsic Microporosity and Covalent Organic Framework for Gas Separation. *J. Membr. Sci.* **2017**, *528*, 273–283.

(16) Ghalei, B.; Sakurai, K.; Kinoshita, Y.; Wakimoto, K.; Isfahani, A. P.; Song, Q.; Doitomi, K.;

Furukawa, S.; Hirao, H.; Kusuda, H.; Kitagawa, S.; Sivaniah, E. Enhanced Selectivity in Mixed Matrix Membranes for CO_2 Capture through Efficient Dispersion of Amine-Functionalized MOF Nanoparticles. *Nat. Energy* **2017**, *2*, 17086.

(17) Mitra, T.; Bhavsar, R. S.; Adams, D. J.; Budd, P. M.; Cooper, A. I. PIM-1 Mixed Matrix Membranes for Gas Separations Using Cost-Effective Hypercrosslinked Nanoparticle Fillers. *Chem. Commun.* **2016**, *52*, 5581–5584.

(18) Wu, X.; Liu, W.; Wu, H.; Zong, X.; Yang, L.; Wu, Y.; Ren, Y.; Shi, C.; Wang, S.; Jiang, Z. Nanoporous ZIF-67 Embedded Polymers of Intrinsic Microporosity Membranes with Enhanced Gas Separation Performance. *J. Membr. Sci.* **2018**, *548*, 309–318.

(19) Wang, Z.; Wang, D.; Zhang, S.; Hu, L.; Jin, J. Interfacial Design of Mixed Matrix Membranes for Improved Gas Separation Performance. *Adv. Mater.* **2016**, *28*, 3399–3405.

(20) Liu, G.; Labreche, Y.; Chernikova, V.; Shekhah, O.; Zhang, C.; Belmabkhout, Y.; Eddaoudi, M.; Koros, W. J. Zeolite-Like MOF Nanocrystals Incorporated 6FDA-Polyimide Mixed-Matrix Membranes for CO_2/CH_4 Separation. *J. Membr. Sci.* **2018**, *565*, 186–193.

(21) Liu, G.; Chernikova, V.; Liu, Y.; Zhang, K.; Belmabkhout, Y.; Shekhah, O.; Zhang, C.; Yi, S.; Eddaoudi, M.; Koros, W. J. Mixed Matrix Formulations with MOF Molecular Sieving for Key Energy-Intensive Separations. *Nat. Mater.* **2018**, *17*, 283–289.

(22) Gao, X.; Zou, X.; Ma, H.; Meng, S.; Zhu, G. Highly Selective and Permeable Porous Organic Framework Membrane for CO_2 Capture. *Adv. Mater.* **2014**, *26*, 3644–3648.

(23) Yang, Y.; Goh, K.; Wang, R.; Bae, T.-H. High-Performance Nanocomposite Membranes Realized by Efficient Molecular Sieving with CuBDC Nanosheets. *Chem. Commun.* **2017**, *53*, 4254–4257.

(24) Jiang, X.; Li, S.; He, S.; Bai, Y.; Shao, L. Interface Manipulation of CO_2–Philic Composite

Membranes Containing Designed UiO-66 Derivatives towards Highly Efficient CO_2 Capture. *J. Mater. Chem. A* **2018**, *6*, 15064–15073.

(25) Liu, X.; Wang, X.; Bavykina, A. V.; Chu, L.; Shan, M.; Sabetghadam, A.; Miro, H.; Kapteijn, F.; Gascon, J. Molecular-Scale Hybrid Membranes Derived from Metal-Organic Polyhedra for Gas Separation. *ACS Appl. Mater. Interfaces* **2018**, *10*, 21381−21389.

(26) Yuan, J.; Zhu, H.; Sun, J.; Mao, Y.; Liu, G.; Jin, W. Novel ZIF-300 Mixed-Matrix Membranes for Efficient CO_2 Capture. *ACS Appl. Mater. Interfaces* **2017**, *9*, 38575–38583.

(27) Rodenas, T.; van Dalen, M.; García-Pérez, E.; Serra-Crespo, P.; Zornoza, B.; Kapteijn, F.; Gascon, J. Visualizing MOF Mixed Matrix Membranes at the Nanoscale: Towards Structure-Performance Relationships in CO_2/CH_4 Separation over NH_2-MIL-53(Al)@PI. *Adv. Funct. Mater.* **2014**, *24*, 249–256.

(28) Kang, Z.; Peng, Y.; Qian, Y.; Yuan, D.; Addicoat, M. A.; Heine, T.; Hu, Z.; Tee, L.; Guo, Z.; Zhao, D. Mixed Matrix Membranes (MMMs) Comprising Exfoliated 2D Covalent Organic Frameworks (COFs) for Efficient CO_2 Separation. *Chem. Mater.* **2016**, *28*, 1277–1285.

(29) Arjmandi, M.; Pakizeh, M. Mixed Matrix Membranes Incorporated with Cubic-MOF-5 for Improved Polyetherimide Gas Separation Membranes: Theory and Experiment. *J. Ind. Eng. Chem.* **2014**, *20*, 3857–3868.

(30) Etxeberria-Benavides, M.; David, O.; Johnson, T.; Łozińska, M. M.; Orsi, A.; Wright, P. A.; Mastel, S.; Hillenbrand, R.; Kapteijn, F.; Gascon, J. High Performance Mixed Matrix Membranes (MMMs) Composed of ZIF-94 Filler and 6FDA-DAM Polymer. *J. Membr. Sci.*, *550*, 198–207.

(31) Shan, M.; Seoane, B.; Rozhko, E.; Dikhtiarenko, A.; Clet, G.; Kapteijn, F.; Gascon, J. Azine-Linked Covalent Organic Framework (COF)-Based Mixed-Matrix Membranes for CO_2/CH_4

Separation. *Chem. - Eur. J.* **2016**, *22*, 14467–14470.

(32) Tien-Binh, N.; Vinh-Thang, H.; Chen, X. Y.; Rodrigue, D.; Kaliaguine, S. Crosslinked MOF-Polymer to Enhance Gas Separation of Mixed Matrix Membranes. *J. Membr. Sci.* **2016**, *520*, 941–950.

(33) Biswal, B. P.; Chaudhari, H. D.; Banerjee, R.; Kharul, U. K. Chemically Stable Covalent Organic Framework (COF)-Polybenzimidazole Hybrid Membranes: Enhanced Gas Separation through Pore Modulation. *Chem. - Eur. J.* **2016**, *22*, 4695–4699.

(34) Wu, H.; Li, X.; Li, Y.; Wang, S.; Guo, R.; Jiang, Z.; Wu, C.; Xin, Q.; Lu, X. Facilitated Transport Mixed Matrix Membranes Incorporated with Amine Functionalized MCM-41 for Enhanced Gas Separation Properties. *J. Membr. Sci.* **2014**, *465*, 78–90.

(35) Paolo, G.; Stefano, B.; Nicola, B.; Matteo, C.; Roberto, C.; Carlo, C.; Davide, C.; Guido, L. C.; Matteo, C.; Ismaila, D.; Andrea Dal, C.; Stefano de, G.; Stefano, F.; Guido, F.; Ralph, G.; Uwe, G.; Christos, G.; Anton, K.; Michele, L.; Layla, M.-S.; Nicola, M.; Francesco, M.; Riccardo, M.; Stefano, P.; Alfredo, P.; Lorenzo, P.; Carlo, S.; Sandro, S.; Gabriele, S.; Ari, P. S.; Alexander, S.; Paolo, U.; Renata, M. W. QUANTUM ESPRESSO: A Modular and Open-Source Software Project for Quantum Simulations of Materials. *J. Phys.: Condens. Matter* **2009**, *21*, 395502.

(36) Perdew, J. P.; Burke, K.; Ernzerhof, M. Generalized Gradient Approximation Made Simple. *Phys. Rev. Lett.* **1996**, *77*, 3865–3868.

(37) Vanderbilt, D. Soft Self-Consistent Pseudopotentials in a Generalized Eigenvalue Formalism. *Phys. Rev. B* **1990**, *41*, 7892–7895.

(38) Rappe, A. K.; Casewit, C. J.; Colwell, K. S.; Goddard, W. A.; Skiff, W. M. UFF, a Full Periodic Table Force Field for Molecular Mechanics and Molecular Dynamics Simulations. *J. Am. Chem. Soc.*

1992, *114*, 10024–10035.

(39) Mayo, S. L.; Olafson, B. D.; Goddard, W. A. DREIDING: A Generic Force Field for Molecular Simulations. *J. Phys. Chem.* **1990**, *94*, 8897–8909.

(40) Benzaqui, M.; Semino, R.; Menguy, N.; Carn, F.; Kundu, T.; Guigner, J.-M.; McKeown, N. B.; Msayib, K. J.; Carta, M.; Malpass-Evans, R.; Le Guillouzer, C.; Clet, G.; Ramsahye, N. A.; Serre, C.; Maurin, G.; Steunou, N. Toward an Understanding of the Microstructure and Interfacial Properties of PIMs/ZIF-8 Mixed Matrix Membranes. *ACS Appl. Mater. Interfaces* **2016**, *8*, 27311–27321.

(41) Plimpton, S. Fast Parallel Algorithms for Short-Range Molecular Dynamics. *J. Comput. Phys.* **1995**, *117*, 1–19.

(42) Abbott, L. J.; Hart, K. E.; Colina, C. M. Polymatic: A Generalized Simulated Polymerization Algorithm for Amorphous Polymers. *Theor. Chem. Acc.* **2013**, *132*, 1334.

(43) Wang, J.; Wolf Romain, M.; Caldwell James, W.; Kollman Peter, A.; Case David, A. Development and Testing of a General Amber Force Field. *J. Comput. Chem.* **2004**, *25*, 1157–1174.

(44) Eggimann, B. L.; Sunnarborg, A. J.; Stern, H. D.; Bliss, A. P.; Siepmann, J. I. An Online Parameter and Property Database for the TraPPE Force Field. *Mol. Simul.* **2014**, *40*, 101–105.

(45) Semino, R.; Moreton, J. C.; Ramsahye, N. A.; Cohen, S. M.; Maurin, G. Understanding the Origins of Metal–Organic Framework/Polymer Compatibility. *Chem. Sci.* **2018**, *9*, 315–324.

(46) Berendsen, H. J. C.; Postma, J. P. M.; Gunsteren, W. F. v.; DiNola, A.; Haak, J. R. Molecular Dynamics with Coupling to an External Bath. *J. Chem. Phys.* **1984**, *81*, 3684–3690.

(47) Todorov, I. T.; Smith, W.; Trachenko, K.; Dove, M. T. DL_POLY_3: New Dimensions in Molecular Dynamics Simulations via Massive Parallelism. *J. Mater. Chem.* **2006**, *16*, 1911–1918.

(48) Allen, M.; Tildesley, D. Oxford University Press; New York: 1987. *Computer simulation of*

liquids.

(49) Kansy, J. Microcomputer Program for Analysis of Positron Annihilation Lifetime Spectra. *Nucl. Instrum. Methods Phys. Res., Sect. A* **1996**, *374*, 235–244.

(50) Tao, S. J. Positronium Annihilation in Molecular Substances. *J. Chem. Phys.* **1972**, *56*, 5499–5510.

(51) Eldrup, M.; Lightbody, D.; Sherwood, J. N. The Temperature Dependence of Positron Lifetimes in Solid Pivalic Acid. *Chem. Phys.* **1981**, *63*, 51–58.

(52) Pascual-Izarra, C.; Dong, A. W.; Pas, S. J.; Hill, A. J.; Boyd, B. J.; Drummond, C. J. Advanced Fitting Algorithms for Analysing Positron Annihilation Lifetime Spectra. *Nucl. Instrum. Methods Phys. Res., Sect. A* **2009**, *603*, 456–466.